ELSEVIER

Chemical Engineering Journal 67 (1997) 215–219

Chemical Engineering Journal

Power consumption of a dual turbine–helical ribbon impeller mixer in ungassed conditions

T. Espinosa-Solares [a,b], E. Brito-De La Fuente [b,c,*], A. Tecante [b], P.A. Tanguy [c]

[a] *Dept. de Ingenieria Agroindustrial, Universidad Autonoma de Chapingo, P.O. Box 161, Chapingo 56230, Edo. de México, México*

[b] *Dept. de Alimentos y Biotecnologia, Facultad de Química, ''E'', UNAM, Mexico City, 04510 México, D.F., México*

[c] *Dept. of Chemical Engineering, Ecole Polytechnique, P.O. Box 6079, Station Centreville, Montreal, Que. H3C 3A7, Canada*

Accepted 14 April 1997

Abstract

Ungassed power measurements in a dual coaxial mixer composed of a helical ribbon and a Rushton turbine were carried out in laminar mixing conditions for Newtonian and non-Newtonian shear thinning fluids. For the Newtonian case, the power draw constant K_p for the hybrid geometry was not the sum of the individual impellers. This was explained by considering the radial discharge flow in the turbine region as well as the top-to-bottom circulation pattern of the helical ribbon impeller. For the non-Newtonian fluids, the results showed that, at a given Reynolds number, power consumption decreases as the shear thinning behaviour increases. A dimensionless and unique representation of the power draw data was obtained by shifting the non-Newtonian power draw results to the Newtonian curve. This was carried out with a K_s function defined from the $K_p(n)$ data. The predictions for K_s were found to be in good agreement with those obtained using the classical method of A.B. Metzner and R.E. Otto (AIChE J., 3 (1957) 3–10). It was observed that pseudoplasticity tends to shift the upper limit of the laminar region toward Reynolds numbers higher than 10. © 1997 Elsevier Science S.A.

Keywords: Viscous mixing; Dual impellers; Power consumption; Non-Newtonian fluids

1. Introduction

Many transformation processes in the food, chemical and fermentation industries involve mixing operations of complex fluid streams such as fibres, suspensions and gels. In mixing, the flow conditions in the mixers are known to govern the process efficiency and the product quality. These flow conditions are particularly sensitive to the non-Newtonian properties (shear-thinning, thixotropy, elasticity) of the media at hand, and the rheological evolution in the vessel due to physical or chemical reactions. Although it is now recognized that for mixing rheologically complex fluids, close clearance impellers are more effective, however, the classical Rushton turbine remains the most common impeller in industrial and research equipment, particularly in the fermentation industry.

Fermenters are usually employed in the production of biomass as well as intra- and extra-metabolites. In these processes, mixing plays a dual role: to ensure the homogenization of nutrients, and also in oxygen transfer. An ideal impeller should mix the bulk efficiently and at the same time promote gas dispersion. It is well known that owing to the evolving rheological properties of many broths, the Rushton turbine does not perform efficiently. Henzler and Obernosterer [1] using Rushton turbines with shear thinning fluids proved that, under ungassed conditions, the dead zones in the agitated vessel could be up to 70%. This problem was attributed to the existence of viscosity gradients in the mixing tank, which are generated by the different shear rates found in the vessel [2]. If mass transfer is considered at the same time, the problem becomes even more severe.

The design of optimal mixers for rheologically evolving systems is still an open issue in industry. Two basic schemes are followed: the most common is to use an impeller which represents the best compromise in terms of mixing efficiency over the course of the reaction; the second is to change the impeller during the process. The latter alternative is in practice difficult to implement and sometimes not recommendable for certain sensitive processes like fermentation.

Another possible approach is the use of combined or hybrid geometry impellers. Although not well documented, several empirical designs have been proposed in the literature which involve combinations of high-speed and low-speed impellers [3].

* Corresponding author.

PII S1385-8947(97)00040-5

Investigations have been carried out in mixing tanks with non-standard geometries. Strek et al. [4] developed a conical impeller in order to promote gas dispersion. The authors concluded that power consumption is lower than that obtained with an equivalent turbine. However, the authors warned that these results could be modified with the presence of two phases (gas–liquid). Pandit [5] proposed an impeller with flinging blades based on a Rushton turbine. The power consumption level was found to be insensitive to the presence of gas. Studies with a dual impeller (Rushton turbine and Scaba impeller) were presented by John et al. [6]. They noted that, by keeping constant the velocity of the Rushton turbine, the total power input is mainly governed by the Scaba impeller. Nouri and Whitelaw [7] reported the flow characteristics of hyperboloid stirrers. The authors observed that this device has a power consumption up to 28 times less than Rushton turbines but that the mixing performance was deficient. Recently, Fort et al. [8] presented an uncommon mixing system consisting of a spherical vessel with a modified anchor impeller. They concluded that the power input depends on the ratio of the immersed area to the total area, and that it is independent of the liquid volume.

The objective in the above studies was to obtain a more efficient geometry than the traditional Rushton turbine. The performance of these new geometries is now relatively well documented for the Newtonian case but there is almost no information regarding their efficiency in the context of rheologically complex fluids.

The aim of the present work is to investigate the mixing performance of a new dual impeller mixer under ungassed conditions with both Newtonian and non-Newtonian fluids. This mixer is composed of a coaxial Rushton turbine and an helical ribbon impeller rotating at different speeds. The helical ribbon impeller was chosen because of its good top-to-bottom pumping characteristics with non-Newtonian fluids and the Rushton turbine owing to its proven capabilities for gas dispersion.

It is worth noting here that this mixing system as well as the operating conditions described in the following section have been designed for aerobic fermentation applications. Parallel work is being carried out by our research group in order to evaluate the gas–liquid mass-transfer capabilities of the system. The results of this study will be reported later.

2. Experimental set-up

The experiments were performed in a flat cylindrical vessel of 0.21 m inner diameter using the double coaxial impeller shown in Fig. 1. The impeller system was fitted to a driving shaft coupled to a variable speed motor. A custom-designed gear box was used to set the speed ratio between the Rushton turbine and the helical impeller. This ratio was kept constant and equal to 1:6.2 (i.e. the Rushton turbine rotates 6.2 times faster than the helical ribbon, both in the clockwise direction). Indeed, in typical fermentation applications the rotational speed of the Rushton turbine is around 0–600 rev min^{-1}, and in chemical reactors helical ribbon rotates at speeds of 0–100 rev min^{-1}. The ratio of the height of the liquid to the height of the helical ribbon impeller was specified at 1.26.

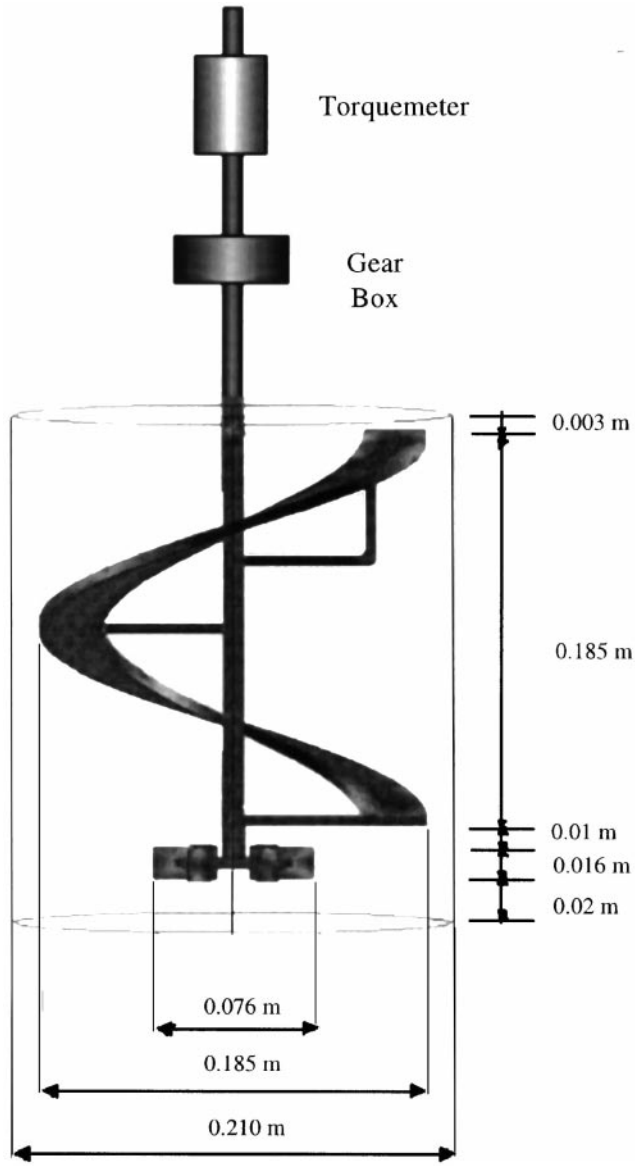

Fig. 1. Experimental set-up.

Six Newtonian corn syrup solutions with viscosities ranging from 3.5 to 71.6 Pa s were used. For the non-Newtonian case, six shear thinning aqueous solutions of Gellan (Kelco, Merck) and xanthan gum (Keltrol T, Kelco-Merck) were studied. Gellan solutions were prepared by adding 0.5% (w/v) of sodium citrate. Xanthan solutions were prepared at constant ionic strength by adding 0.1% (w/v) NaCl. The steady shear viscosity function was evaluated using a rotational rheometer (HAAKE CV-20N) provided with a cone and plate geometry (PK20-4). The viscosity for the shear thinning fluids in the linear region, was well fitted by the Ostwald–de Waele model. The flow behaviour index n ranged

from 0.25 to 1.0 and the consistency index m from 2.8 to 21.5 Pa s^n.

In order to determine the power consumption, torque measurements were performed with a non-contact strain gauge torquemeter (S. Himmelstein Co., model 2081T) in the range from 0 to 2.8 N m, with an accuracy of 0.1% at full scale. The speed of the Rushton turbine was measured with an optical encoder, and with a digital tachometer in the case of the helical ribbon (this last for verification purposes). Experiments were carried out at room temperature.

3. Results and discussion

3.1. Newtonian fluids

We first show in Fig. 2 the experimental results for the Newtonian power consumption. The power constant K_p of the dual mixer can be expressed as

$$N_p \mathrm{Re} = K_p = 340.45 \pm 3.4 \quad (1)$$

It can be seen that the mixing regime for the Newtonian fluids is laminar, since a straight line of slope -1 can be plotted in the whole range of Reynolds number covered in the experiments. It is worth noting that the helical ribbon diameter and rotational speed were used as the characteristic length and velocity respectively in the definition of the Reynolds number.

Power draw measurements carried out on each individual impeller showed that the individual power constant K_p is 138.8 and 72.0 for the helical ribbon and the Rushton turbine respectively. The power curve of these impellers values is also shown in Fig. 2. As can be noticed, the power consumption for the hybrid system is not the sum of the individual impeller contributions. Although it is very difficult to compare these results with data from the literature, an explanation may however be found in the flow pattern created by this dual geometry. Tanguy et al. [9], from three-dimensional numerical simulations on the same geometry, reported a significant rearrangement of the flow pattern in the lowest half of the helical ribbon region due to the action of the turbine. The strong radial discharge flow in the turbine region almost completely offsets the axial pumping of the helical ribbon, resulting in an increase in the energy consumption. For other dual impeller mixing systems (i.e. dual Rushton turbines), total power input is strongly dependent on the impeller spacing and therefore, the induced flow pattern. Höcker et al. [10] concluded that, for dual Rushton turbines, in the turbulent regime, the total power draw is the sum of the individual impeller contributions. However, for the laminar regime, total power is about 20% more than the sum of the individual impeller power consumption.

3.2. Non-Newtonian fluids

Experimental power draw results for the shear thinning fluids are treated as a departure from the Newtonian case. Then, a generalization of the classic dimensionless power draw relation for power law fluids is given by

$$K_p(n) = N_p \, \mathrm{Re}_{gen} = \frac{P}{d^3 N^{1+n} m} \quad (2)$$

The above equation assumes as a characteristic velocity the product of the impeller diameter and the rotational speed Nd, in this case both from the helical ribbon. Fig. 3 shows the experimental results for the shear thinning fluids studied here. As can be seen, for a given Re number, power consumption decreases as a function of the level of pseudoplasticity, and this decrease is more pronounced for the more extreme fluids.

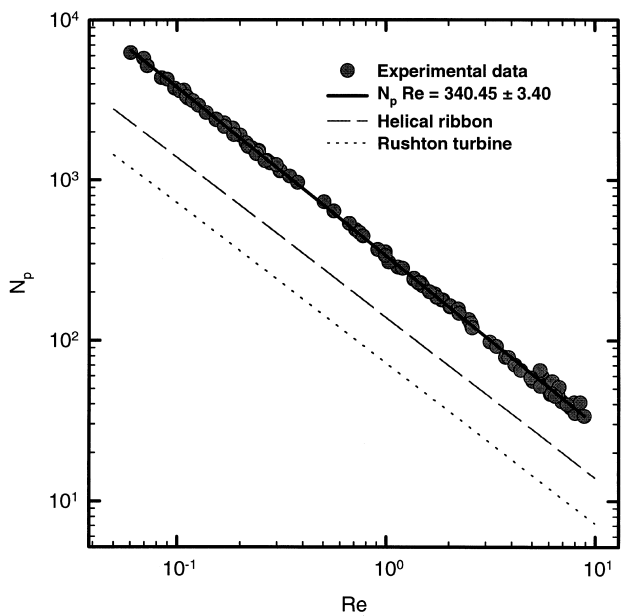

Fig. 2. Newtonian power consumption curve for the hybrid geometry, the helical ribbon and the Rushton turbine.

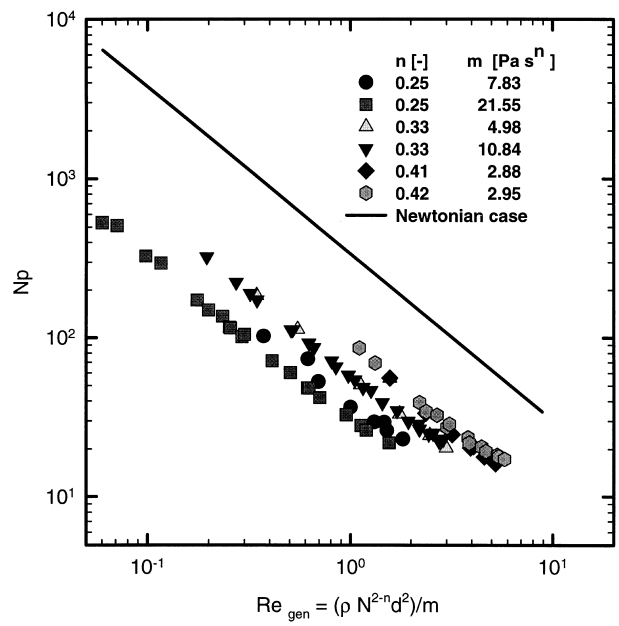

Fig. 3. Non-Newtonian power consumption curve.

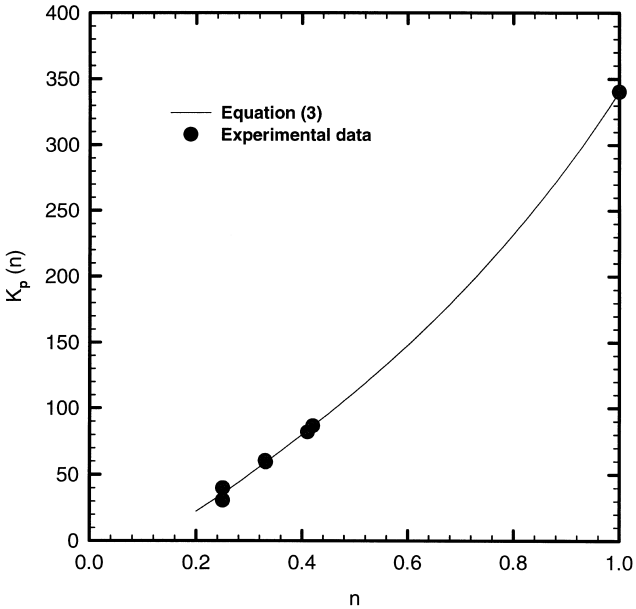

Fig. 4. Experimental $K_p(n)$ data and predicted values from Eq. (3).

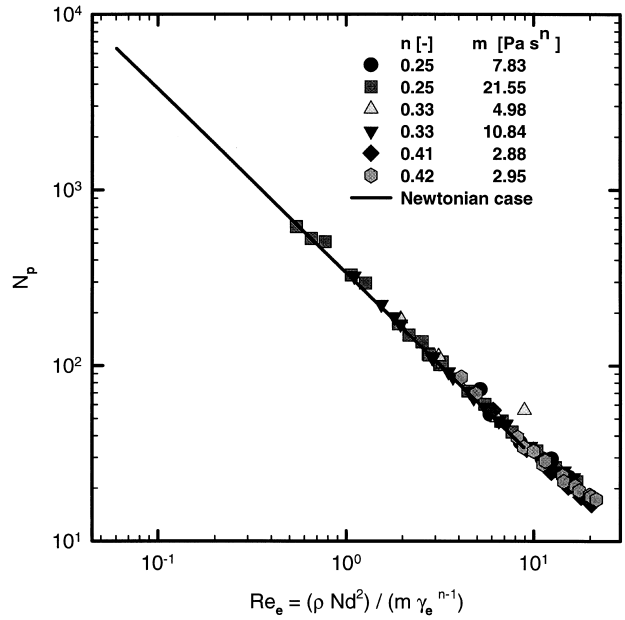

Fig. 5. Generalized dimensionless power consumption curve for the dual helical ribbon–Rushton turbine system.

It must be noted that the results shown in Fig. 3 allow us to estimate the variation of K_p as a function of n. This variation is presented in Fig. 4 for each shear thinning fluid tested. The experimental results were fitted by a non-linear regression algorithm to the following model, as suggested by Brito-De la Fuente et al. [11]:

$$K_p(n) = K_{p(n=1)}\, b^{n-1} c^{(n-1)/n} \tag{3}$$

where the value of $K_{p(n=1)}$ is given by Eq. (1), b and c are equal to 4.19 ± 0.79 and 1.48 ± 0.095 respectively. The plot of Eq. (3) is also shown in Fig. 4. The fitting obtained is very good. Let us mention here that Eq. (2) has been used in the literature to process experimental power draw data obtained with different impeller geometries [11,12].

In order to obtain a generalized dimensionless power draw curve for both Newtonian and non-Newtonian fluids, an effective viscosity (also named process viscosity) η_e must be defined, which is a function of the effective shear rate $\dot{\gamma}_e$. Based on the concepts of Metzner and Otto [13], as well as Eq. (2), Brito-De la Fuente et al. [11] showed that

$$N_p = K_p \frac{\rho N d^2}{\eta_e} = \frac{K_p \rho N d^2}{m(K_s N)^{n-1}} \tag{4}$$

or

$$N_p = \frac{K_p K_s^{n-1}}{(\rho N^{2-n} d^2/m)} = \frac{K_p K_s^{n-1}}{\mathrm{Re}_{gen}} \tag{5}$$

Then, $\dot{\gamma}_e$ can be defined by

$$\dot{\gamma}_e = \left[\frac{K_p(n)}{K_p}\right]^{1/(n-1)} N \tag{6}$$

This effective shear rate is then used to calculate the effective viscosity and thus the effective Reynolds number Re_e, given by

$$\mathrm{Re}_e = \frac{\rho N d^2}{m(\dot{\gamma}_e)^{n-1}} \tag{7}$$

The power input data for the shear thinning fluids were recalculated by using Eq. (7). The results are shown in Fig. 5. As can be observed, the power input results for the non-Newtonian fluids are superimposed on the Newtonian curve. This suggests that the factor used to generalize the results is adequate.

A tendency to shift the upper limit of the laminar region towards higher Re numbers ($\mathrm{Re} > 10$) owing to the shear thinning behaviour is also observed. This is in agreement with previous reports [11,13].

It should be pointed out here that the proportionality factor between the effective rate of deformation and the impeller rotational speed in Eq. (6), is nothing but the well known K_s factor from the Metzner and Otto [13] method, given here by

$$K_s = \left[\frac{K_p(n)}{K_p}\right]^{1/(n-1)} \tag{8}$$

Then, from Eq. (8), it is obvious that the value of K_s depends on the model used to express the $K_p(n)$ results.

Rieger and Novák [14] expressed their power draw results with shear thinning fluids and helical impellers by

$$K_p(n) = K_{p(n=1)} \exp[-B(1-n)] \tag{9}$$

where B is a constant equal to 36.73. If Eq. (9) is substituted into Eq. (8), then the resulting K_s is a constant. Netušil and Rieger [12] using shear thinning fluids with n in the range from 0.16 to 1.0, fitted their power consumption results obtained with helical ribbons, screw with a draught tube and off-centered screw by

$$K_p(n) = K_{p(n=1)} n^{\alpha} \tag{10}$$

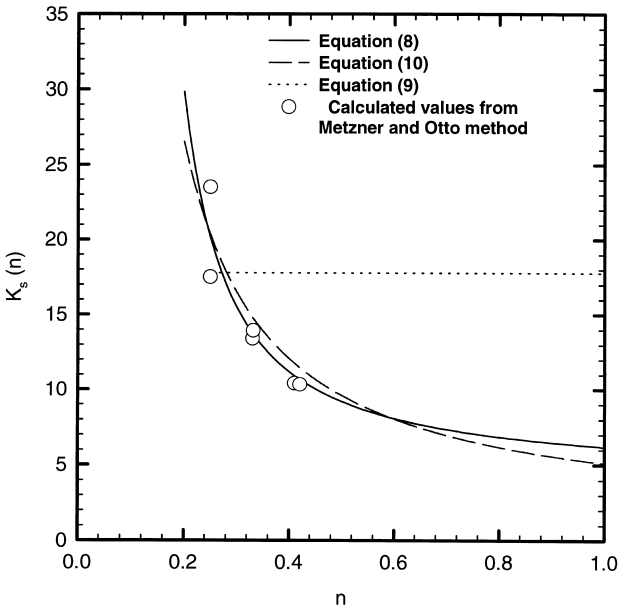

Fig. 6. K_s values from the experimental $K_p(n)$ data and the Metzner–Otto approach.

where α is a constant dependent on the geometry. Again, if this model is substituted into the K_s equation, the result is a decreasing function of n with high K_s values at low values of n. Although the authors proposed Eq. (10), they concluded that an average value of K_s may be used. In Fig. 6, we show the predicted results for the K_s parameters using our experimental results expressed by Eq. (3) as well as the estimated values obtained by following the classic Metzner and Otto [13] calculation. It is clear that K_s is a function of the fluid flow properties regardless of the model used to express the power input data. Let us emphasize that one advantage of using Eq. (6) is that there is no need to know a priori a K_s value. Furthermore, if needed, K_s can be determined with a reasonable accuracy using only one power input measurement and Eq. (2), in addition to the Newtonian power curve.

4. Nomenclature

b	constant in Eq. (3)	(–)
c	constant in Eq. (3)	(–)
d	impeller diameter	(m)
K_p	$K_p = \mathrm{Re}N_p$	(–)
$K_p(n)$	defined by Eq. (2)	(–)
K_s	defined by Eq. (6)	(–)
m	consistency index in the power law model	(Pa s^n)
n	flow behaviour index in the power law model	(–)
N	rotational speed of impeller	(rev s^{-1})
N_p	power number of impellers, $N = P/\rho d^5 N^3$	(–)
P	power consumption of impeller	(W)
Re_e	effective Reynolds number, $\mathrm{Re}_e = \rho N d^2/m\gamma_e^{n-1}$	(–)
Re_{gen}	generalized Reynolds number, $\mathrm{Re}_{gen} = \rho N^{2-n} d^2/m$	(–)
μ	viscosity	(Pa s)
ρ	density	(kg m^{-3})
$\dot{\gamma}_e$	effective shear rate given by Eq. (6)	(s^{-1})

Acknowledgements

The authors wish to acknowledge the financial support provided by the National Council of Science and Technology of Mexico (CONACyT) and DGAPA-UNAM (Mexico).

References

[1] H.J. Henzler, G. Obernosterer, Chem. Eng. Technol. 14 (1991) 1–10.
[2] M. Kamiwano, F. Saito, M. Kaminoyama, Int. Chem. Eng. 30 (2) (1990) 274–280.
[3] M.F. Edwards, M.R. Baker, A review of liquid mixing equipment, in: N. Harnby, M.F. Edwards, A.W. Nienow (eds.), Mixing in the Process Industries, Butterworth-Heinemann, 1992, pp. 118–136.
[4] F. Strek, J. Karcz, W. Bujalski, Chem. Eng. Technol. 13 (1990) 384–392.
[5] A.B. Pandit, Trans. IChemE. A 71 (1993) 444–452.
[6] A.H. John, W. Bujalski, A.W. Nienow, A. Sánchez, L. Torres, E. Galindo, Trans. IChemE. A 73 (1995) 535–541.
[7] J.M. Nouri, J.H. Whitelaw, Can. J. Chem. Eng. 72 (1994) 782–791.
[8] I. Fort, M. Poux, P. Fayolle, J. Bertrand, Trans. IChemE. A 72 (1994) 455–460.
[9] P.A. Tanguy, F. Thibault, E. Brito-De La Fuente, T. Espinosa, A. Tecante, Mixing performance induced by coaxial flat blade-helical ribbon impellers rotating at different speeds, submitted to Chem. Eng. Sci. (1996).
[10] H. Höcker, G. Langer, U. Werner, Ger. Chem. Eng. 4 (1981) 113–123.
[11] E. Brito-De la Fuente, J.C. Leuliet, L. Choplin, P.A. Tanguy, AIChE Symp. Ser. 286 (1992) 88, 28–32.
[12] J. Netušil, F. Rieger, Chem. Eng. J. 52 (1993) 9–12.
[13] A.B. Metzner, R.E. Otto, AIChE J. 3 (1) (1957) 3–10.
[14] F. Rieger, V. Novák, Trans. IChem E. 51 (1973) 105–111.